Low-Thrust Orbit Transfers Between Two-Body Keplerian Orbits

Mariana Sá*
Nonlinear Dynamics Group, Departamento de Física, Instituto Superior Técnico − IST, Universidade de Lisboa − UL, Avenida Rovisco Pais 1, 1049, Lisboa, Portugal
(Dated: January 11, 2021)

We developed a new algorithm for a general satellite transfer between two Keplerian orbits in the same plane where we controlled the three constants of motion of the Kepler problem, using a *bang-bang* control. During transfers, the orbits are no longer Keplerian and the final orbit is reached by varying the constants of motion along them. We simulated transfers between elliptical, hyperbolic, and circular orbits with constant angular momentum, with constant effective energy, and with both variable angular momentum and effective energy. Furthermore, we studied a particular case of transfers: between two circular orbits, and used the Laplace-Runge-Lenz vector to rotate the orientation of the lines of apsides.

I. Introduction

In the latter half of the twentieth century, rockets were developed and overcame the gravity force, beginning the era of space exploration. However, there is still much work to do regarding space exploration and a fundamental part of that is the application of orbital maneuvers, i.e., the transfer of a spacecraft or satellite between orbits. An example is a set of GPS satellites in which one of them crashed and it is necessary to replace it, sending another satellite to its position.

This is a problem of high complexity and many new strategies of transfers have been developed, involving optimization criteria to minimize the costs and the transfer time. The first studies in the field appeared around 1960 ([1–3] as examples). Nowadays, the trajectory optimization problem is still a subject studied by the scientific community and many techniques using different methods have been implemented [4–6].

To transfer a spacecraft between two orbits, it is necessary to change its velocity, which is done through the burning of rocket engines on the spacecraft. To do that we have two types of maneuvers: the impulsive and the non-impulsive. The difference between them is that the former consists of instantaneous burn fires with high-thrust chemical propulsion systems at some chosen points of the orbit, while in the latter the burn fires are applied during a longer time period. The main example of impulsive maneuvers is the Hohmann transfers [7], while low-thrust transfers are examples of non-impulsive.

Initially, only impulsive maneuvers were carried out, but the situation changed with the appearance of ionic motors and others in the 1960s [8]. These new technologies are very efficient, with a specific impulse several times higher than chemical propulsion, but with a smaller force, which implies that to be useful they have to work for long periods of time, i.e., continuously. Some more recent examples of satellites that use electric thrusters are documented in [9–11].

The main goal of this master thesis is to develop a new algorithm for plane transfers based on the control and optimization of the constants of motion of the Kepler problem. These constants are angular momentum and Laplace-Runge-Lenz (LRL) vectors and energy. This project is an extension of [12], where 2-dimensional transfers with constant angular momentum and with constant effective energy have already been considered. In this thesis, we have extended these techniques to all possible Keplerian orbits, eliminating convergence problems and situations where non reachable targets exist. The main results of this thesis are exposed in [13].

II. Mathematical Formalism

The spacecraft or satellite motion is approximated by that of a variable mass point, subject to the gravitational attraction of one primary massive body (the center of gravitational force) with mass M. We consider that the motion is described in a two-dimensional configuration space with coordinates $(x,y) \in \mathbb{R}^2$. The satellite has mass m and it has its own propulsion system which, when turned on, causes spacecraft to lose mass and gain speed. Therefore, the equation of motion is given by

$$m\frac{d^2\vec{r}}{dt^2} - \frac{dm}{dt}\vec{u}_{rel} = -\frac{GmM}{r^3}\vec{r}, \tag{1}$$

where $\vec{r} = (x,y) \in \mathbb{R}^2$, G is the universal gravitational constant and $\vec{u}_{rel} = (u_x, u_y)$ is the velocity of the mass lost by the satellite measured in its referential frame. If we assume a satellite with a large mass compared to the mass lost by the propulsion system we make the approximation

$$\frac{1}{m}\frac{dm}{dt} = \gamma, \tag{2}$$

where $\gamma < 0$ is a constant. Initially, the propulsion system is off, $\vec{u}_{rel} = 0$, but when it is turned on we have that

$$(u_x, u_y) = (u\cos\phi, u\sin\phi), \tag{3}$$

where ϕ is the escape angle of the satellite.

The system of equations resulting from the substitution of (2) in (1) is derived from the time-dependent Lagrangian

$$\mathscr{L} = \frac{1}{2}\left(\dot{x}^2 + \dot{y}^2\right) + \frac{\mu}{r} + \gamma x u_x + \gamma y u_y, \tag{4}$$

where $\mu = GM$.

To simplify the parametric dependence of these equations, we introduce new radial and temporal variables $s = \frac{r}{r_0}$ and $\tau = \zeta t$, where r_0 and ζ are constants to be determined below.

* mariana.sa@tecnico.ulisboa.pt

Then, by equation (4), the new Lagrangian becomes

$$\mathscr{L} = \zeta^2 r_0^2 \left[\frac{1}{2}\left(\dot{s}^2 + s^2\dot{\theta}^2\right) + \frac{\mu}{r_0^3\zeta^2}\frac{1}{s} + \frac{\bar{\gamma}}{r_0} s\left(\bar{u}_x\cos\theta + \bar{u}_y\sin\theta\right)\right], \tag{5}$$

where now the dot ($\dot{}$) denotes the derivative with respect to τ, $\gamma = \zeta\bar{\gamma}$, $u_{x,y} = \zeta\bar{u}_{x,y}$ and we use polar coordinates, $(x,y) = (r\cos\theta, r\sin\theta)$. Choosing $\zeta^2 r_0^2 = 1$ and $\mu/(r_0^3\zeta^2) = 1$, we obtain $\zeta = 1/\mu$ and $r_0 = \mu$. Introducing the definitions of u_x and u_y in equation (3), the rescaled radial variable and the control parameter $\varepsilon = \bar{\gamma}\bar{u}/r_0 = \mu^3\gamma u$ into equation (5), we finally obtain the control equations

$$\begin{cases} \ddot{s} = \frac{L_z^2}{s^3} - \frac{1}{s^2} + \varepsilon\cos(\theta-\phi) \\ \frac{d}{d\tau}L_z = -\varepsilon s\sin(\theta-\phi) \end{cases}, \tag{6}$$

where $L_z = s^2\dot{\theta}$ is the angular momentum of the satellite. The satellite is under control only if $\varepsilon \neq 0$ (< 0). Otherwise, equations (6) describe the Keplerian trajectory of the satellite in the two-dimensional rescaled configuration space.

Using the Lagrangian and Hamilton's equations we obtain the total energy of the satellite. The Hamiltonian becomes

$$H = \frac{1}{2}\left(\dot{s}^2 + \frac{L_z^2}{s^2}\right) - \frac{1}{s} - \varepsilon s\cos(\theta-\phi). \tag{7}$$

When the control is turned on,

$$\frac{dH}{d\tau} = \varepsilon\left[\dot{s}\cos(\theta-\phi) - s\dot{\theta}\sin(\theta-\phi)\right], \tag{8}$$

and we conclude that the energy is not conserved.

The third constant of motion is the LRL vector [14]. This vector describes the shape and the orientation of an orbit and is defined mathematically by the formula[1]

$$\vec{A} = \dot{\vec{s}}\times\vec{L} - \frac{\vec{s}}{s}, \tag{9}$$

which corresponds to

$$\vec{A} = \left(\dot{\bar{y}}L_z - \frac{\bar{x}}{s}\right)\hat{x} - \left(\dot{\bar{x}}L_z - \frac{\bar{y}}{s}\right)\hat{y}, \tag{10}$$

for an orbit on the xy plane, where $\vec{s} = (\bar{x},\bar{y}) = (x,y)/r_0$ and $\hat{x}$ and $\hat{y}$ are the usual Cartesian versors.

In most transfers, the final orbit has a different orientation than the initial one. Thus, the rotation between the two orbits is another parameter that we intend to analyze and this is done using the LRL vector. In section VII we find a detailed analysis of the process to obtain orbits with the same orientation.

In this thesis, we only consider transfers between orbits with positive angular momentum ($L_z > 0$). Thus, the trajectories are counterclockwise in the configuration space and clockwise in the phase space. The case $L_z < 0$ can be solved by a different choice (orientation) of the Cartesian reference frame and $L_z = 0$ correspond to collision trajectories.

The energy has a local minimum for the circular orbit, which corresponds to the fixed point $(s^*, \dot{s} = Lz^2, 0)$. This implies that the regions with energies below this minimum value are inaccessible. Therefore, $H \in [H(s^*), +\infty]$. This will be analyzed in section VI. While points with $H < 0$ and $H = 0$ correspond to elliptical and parabolic orbits, respectively, points with $H > 0$ correspond to hyperbolic escape trajectories. In this work, we consider transfers between elliptical, circular, and hyperbolic orbits.

According to reference [12], there is a critical value for ε, $\varepsilon_{lim} = -\frac{4}{27}$. If $\varepsilon \leq \varepsilon_{lim}$, the orbits in phase space are always open, so we consider $\varepsilon > \varepsilon_{lim}$ and, for the simulations, we choose $\varepsilon = -0.1$, just like the one chosen in that reference. As ε increases, transfers take longer to be completed.

Throughout this project, we use the 4^{th} order Runge-Kutta numerical integration method built-in NDSolve of *Mathematica- version 12.2*. In addition, we resort to the **WhenEvent**[*event, action*] [2] command to impose control conditions. This command simplifies the writing and reading of the program since it specifies an action when the event is detected in NDSolve.

III. Transfers with constant angular momentum

In this section, we are going to study transfers between Keplerian orbits with constant angular moment, but different effective energies. In other words, the satellite is initially in an orbit with a certain angular momentum L_{z0} and a certain effective energy H_0 and we need to transfer it to another orbit with the same angular momentum $L_{zf} = L_{z0}$ but with a different effective energy H_f. Transfers start at time $\tau = 0$, with effective energy H_0, and stop when the final effective energy H_f is reached. These transfers are carried out under very specific control conditions, which are presented below.

Since the angular momentum must be constant throughout the transfers ($dL_z/d\tau = 0$), by the second equation of (6), we must impose that $\sin(\theta-\phi) = 0$ and we obtain two control conditions: $\phi = \theta$ or $\phi = \theta \pm \pi$. The system of equations (6) and equation (8) are rewritten as:

$$\begin{cases} \ddot{s} = \frac{L_z^2}{s^3} - \frac{1}{s^2} + \varepsilon\sigma \\ \dot{\phi} = \dot{\theta} = \frac{L_z}{s^2} \\ \dot{H} = \varepsilon\sigma\dot{s}, \end{cases} \tag{11}$$

where $\varepsilon = -0.1$ is a fixed value and $\cos(\theta-\phi)$ is replaced by σ, which can take the values ± 1 or also 0 (when the control parameter is off for sake of simplification), according to each imposed condition.

There are two types of transfers: i) $H_f > H_0$ and ii) $H_f < H_0$. To the first case, $dH/d\tau > 0$, from the last equation of (11) we have that if $\dot{s} > 0$ implies that $\sigma = -1$ and if $\dot{s} \leq 0$, $\sigma = 1$. However, according to the orbital phase space, these conditions are sufficient only for this case ($H_f > H_0$). When

[1] Note that here we defined this vector per mass unit and now it is dimensionless.

[2] https://reference.wolfram.com/language/ref/WhenEvent.html

the effective energy decreases along with the transfer, we must be careful with the geometry of the orbits. First, we have to calculate the fixed points corresponding to each control parameter $\sigma = 0$ and ± 1. To do that, we make a variable change in the first equation of (11) such that $\dot{s} = y$ and, therefore, the fixed points are given by solving

$$\dot{y} = 0 \Rightarrow \frac{L_z^2}{s^3} - \frac{1}{s^2} + \sigma\varepsilon = 0, \tag{12}$$

in order to s. Based on Figure 4.3 from reference [15], we classify the fixed points depending on σ value. When $\sigma = 0$, there is one fixed point which coincides with the circular orbit with radius $s_0^* = L_z^2$ and, consequently, with the minimum effective energy, $H_0 = H(s_0^*, 0) = -1/(2L_z^2)$. This fixed point is Lyapunov stable and center type. When $\sigma = 1$, equation (12) has three solutions but only one is real, s_1^*, and corresponds to a fixed point which is also Lyapunov stable and center type. The case where $\sigma = -1$ is more complicated because it depends on the chosen ε and L_z values. In this work, as $\varepsilon = -0.1$, there are always three solutions depending on the L_z value:

- if $L_z > L_{zlim} = 1.1033$, only one of the solutions is real but negative, which implies that there are no fixed points;
- if $L_z \leq L_{zlim}$, the three solutions are real but only two are positive and correspond to the fixed points, s_{-1}^* and s_{-2}^*, where $s_{-2}^* > s_{-1}^*$. s_{-1}^* is Lyapunov stable and center type and s_{-2}^* is unstable and saddle type.

After studying the phase spaces for each value of the control parameter and verifying that there are no fixed points when $\sigma = -1$ and $L_z > L_{zlim}$, we conclude that using this control choice transfers would be limited by a certain angular momentum value: $L_z \leq L_{zlim}$. As we intend to obtain transfers regardless of the final angular momentum value, we have to ignore this control parameter and, through the last equation of system (11), make the control choices: $\sigma = 1$ if $\dot{s} > 0$ and $\sigma = 0$ if $\dot{s} \leq 0$. Thus, the control conditions for the two possible cases of transfers with constant angular momentum are summarized in Table I.

	$\dot{s} \leq 0$	$\dot{s} > 0$
$\dot{H} > 0$	$\sigma = 1$	$\sigma = -1$
$\dot{H} < 0$	$\sigma = 0$	$\sigma = 1$

Table I. Final control conditions for transfers with constant angular momentum.

Despite that, if we look closely at the orbital phase spaces overlapping with $\sigma = 0$ and $\sigma = 1$, we find that in the region between the fixed points there must be a specific control choice condition when $H_0 > H_f$ because it is problematic when the satellite final orbit has to be circular. In this region, the solution to this problem is to leave the control off when $\dot{s} = 0$. The satellite will remain in the same orbit (with $\sigma = 0$) and the control will only be switched on again when that orbit intersects another orbit with $\sigma = 1$ and that leads us to the desired effective energy. The intersection between the orbits with $\sigma = 0$ with $\sigma = 1$ occurs when

$$s = s_i = \frac{L_z^2}{2\varepsilon s_a^2} - \frac{1}{\varepsilon s_a} + \frac{1}{2\varepsilon L_z^2} + L_z^2, \tag{13}$$

where s_a is the s value when $\dot{s} = 0$ and σ remains off.

case	L_z	orbit geometry	initial conditions	H_f	$\Delta\tau$
ii)	1.3	elliptic to elliptic	$s_0 = 4$ $\dot{s}_0 = 0$ $\theta_0 = 0$ $H_0 = -0.1972$	-0.25	14.8
i)	1.4	circular to hyperbolic	$s_0 = 1.96$ $\dot{s}_0 = 0$ $\theta_0 = \frac{3\pi}{2}$ $H_0 = -0.2551$	0.2	11.7
i)	0.8	hyperbolic to hyperbolic	$s_0 = 0.3022$ $\dot{s}_0 = -0.1$ $\theta_0 = \frac{\pi}{2}$ $H_0 = 0.2$	0.5	2.4
ii)	1	hyperbolic to circular	$s_0 = 0.4589$ $\dot{s}_0 = -0.1$ $\theta_0 = \pi$ $H_0 = 0.2$	-0.5	45.8

Table II. Examples of transfers with constant angular momentum. Note that all quantities are dimensionless, except the polar angle θ_0 which is measured in radians.

Some examples of transfers involving circular, elliptical, and hyperbolic orbits are summarized in Table II, where $\Delta\tau$ is a dimensionless transfer time.

Let us consider the first example in Table II: a transfer between two elliptical orbits with initial and final effective energies of $H_0 = -0.197188$ and $H_f = -0.25$, respectively. This is depicted in Figure 1 and the angular momentum is purposely chosen as $L_z = 1.3 > L_{zlim}$ to prove that with the two controls parameters described in Table I it is possible to obtain transfers with decreasing effective energy for angular momentum values greater than the limit value that we would have if we used the control parameter $\sigma = -1$. In the first two plots of this figure are represented the phase and the configuration spaces of the satellite trajectory. In the two plots below, we see the control choice variation that is made using the data from Table I as well as the effective energy variation during the entire transfer. We conclude that in fact we can obtain transfers without the control parameter $\sigma = -1$ and ensuring that transfers occur regardless of the chosen L_z value. However, the control remains zero during almost the entire transfer and, consequently, this increases the transfer time.

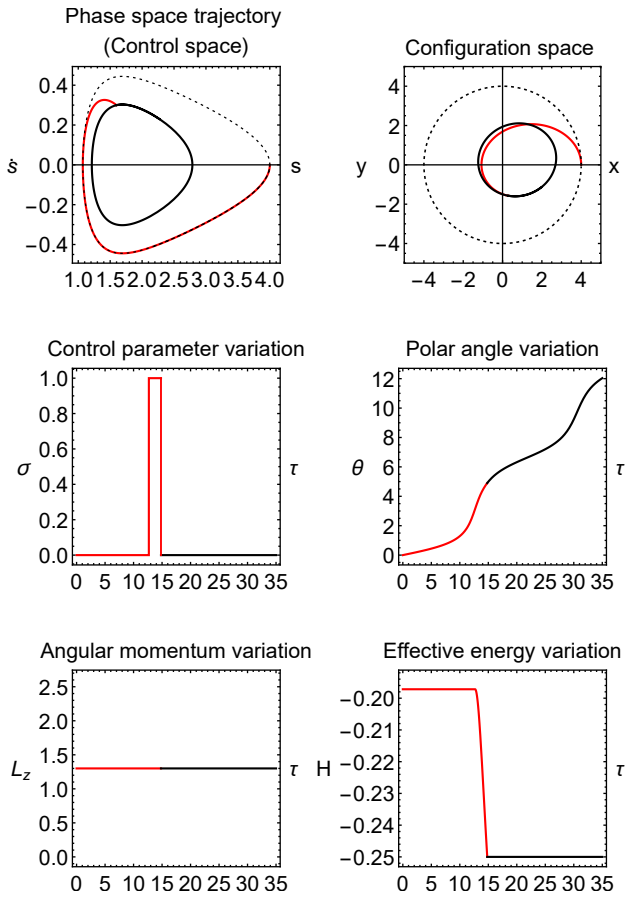

Figure 1. Simulation of a transfer with constant angular momentum ($L_z = 1.3$) between two elliptical orbits: the initial with an effective energy ($H_0 = -0.1972$) and the final with ($H_f = -0.25$). The initial orbit is represented by the dashed line, the transfer by red and the final orbit by black. The transfer starts at the point $(s_0, \dot{s}_0, \theta_0) = (4, 0, 0)$ and takes a normalized time $\Delta\tau = 14.8$ to be completed.

IV. Transfers with constant effective energy

We now consider transfers with constant effective energy, which start at time $\tau = 0$ with angular momentum L_{z0} and stop when the final angular momentum value L_{zf} is reached. We also consider that the initial and final values of angular momentum have the same sign (in this case, the plus sign) so that during a transfer the value of the angular momentum is never zero.

If we equal the equation (8) to zero we have the control condition corresponding to energy conservation ($\dot{H} = 0$) which is given by

$$\phi = \theta - \arctan\frac{\dot{s}}{s\dot{\theta}}, \tag{14}$$

where $\dot{\theta} = L_z/s^2$. From here, we can obtain the expressions for $\sin(\theta-\phi)$ and $\cos(\theta-\phi)$ which are given by

$$\begin{cases} \sin(\theta-\phi) = \frac{s\dot{s}}{\sqrt{s^2\dot{s}^2+L_z^2}} \\ \cos(\theta-\phi) = \frac{|L_z|}{\sqrt{s^2\dot{s}^2+L_z^2}} \end{cases}, \tag{15}$$

and rewrite the equations of motion (6):

$$\begin{cases} \ddot{s} = \frac{L_z^2}{s^3} - \frac{1}{s^2} + \varepsilon\sigma\sigma_c\frac{|L_z|}{\sqrt{L_z^2+s^2\dot{s}^2}} \\ \frac{d|L_z|}{dt} = -\varepsilon\sigma\sigma_c\frac{s^2\dot{s}}{\sqrt{L_z^2+s^2\dot{s}^2}} \end{cases}, \tag{16}$$

where $\sigma_c = 1$ and σ can take the values ±1 or also 0 (when the control parameter is off for sake of simplification), according to each imposed condition.

If $L_{z0} > L_{zf}$, we must have $H \geq -1/(2L_{z0}^2)$, and if $L_{z0} < L_{zf}$, then $H \geq -1/(2L_{zf}^2)$. This will be better understood in section VI. Therefore, we can consider two types of transfers: i) $L_{z0} > L_{zf}$ and ii) $L_{z0} < L_{zf}$. Similar to transfers of the previous chapter, the case i) has no problems and the control conditions are

$$L_{z0} > L_{zf}: \begin{cases} \text{if } \dot{s} < 0 \wedge L_{z0} > L_{zf} \Rightarrow \sigma = 1 \\ \text{if } \dot{s} \geq 0 \wedge L_{z0} > L_{zf} \Rightarrow \sigma = -1 \\ \text{otherwise } \Rightarrow \sigma = 0 \end{cases}. \tag{17}$$

For the case ii), it is necessary to analyze the geometry of the orbits. To calculate the fixed points, we have to write the expression of $\ddot{s}$ as a function of H, because we are considering transfers with constant effective energy. To do this, we solve the expression (7) with $\varepsilon = 0$ in order to L_z^2 and substitute it in the first of equation (16):

$$\ddot{s} = -\frac{1}{s^2} + \frac{2Hs^2+2s-\dot{s}^2s^2}{s^3} + \sigma\varepsilon\frac{L_z}{\sqrt{L_z^2+s^2\dot{s}^2}}. \tag{18}$$

Then, we do a variable transformation, $\dot{s} = y$, and the fixed points are given by solving

$$\dot{y} = 0 \Rightarrow -\frac{1}{s^2} + \frac{2Hs^2+2s}{s^3} + \sigma\varepsilon = 0, \tag{19}$$

in order to s, where $\dot{s} = 0$, according to each σ value.

When the control parameter is turned off, the fixed point is $(s_0^*, \dot{s}) = (-\frac{1}{2H}, 0)$. When $\sigma = \pm1$, there are two solutions to each case but only one corresponds to a fixed point, depending on the chosen H value. These fixed points are called s_1^* and s_{-1}^* according to the σ value. All the fixed points are Lyapunov stable of center type [15].

However, to s_{-1}^*, there is a limitation in the effective energy values. If $H^2 < |\varepsilon|$, the s^* values are complex and there are no fixed points. Again, similar to what was done in the previous chapter, to overcome this obstacle and since we intend to obtain transfers regardless of the final effective energy value, we ignore the control parameter $\sigma = -1$. Thus, by the last equation of system (16), we choose the control conditions: $\sigma = 1$ if $\dot{s} > 0$ and $\sigma = 0$ if $\dot{s} \leq 0$.

Despite that, if we overlap the orbital phase spaces with $\sigma = 0$ and $\sigma = 1$, we find a problematic region between the fixed points ($s_1^* \leq s \leq s_0^*$), which prevents us from transferring the satellite to a circular orbit. Therefore, we have to implement a new strategy for transfers with $H < 0$ and $L_{z0} < L_{zf}$: firstly, we transfer the satellite to an almost circular orbit with constant energy (until $s_1^* \leq s \leq s_0^*$ and $\dot{s} = 0$) and then we make

case	H	orbit geometry	initial conditions	L_{zf}	$\Delta\tau$
i)	0.2	hyperbolic to hyperbolic	$s_0 = 0.3$ $\dot{s}_0 = 0$ $\theta_0 = 0$ $L_{z0} = 0.79693$	0.2	3.0
i)	-0.5	circular to elliptic	$s_0 = 1$ $\dot{s}_0 = 0$ $\theta_0 = 0$ $L_{z0} = 1$	0.4	15.0
ii)	-0.2	elliptic to elliptic	$s_0 = 0.1878$ $\dot{s}_0 = -0.2$ $\theta_0 = \pi$ $L_{z0} = 0.6$	1	2.9
ii)	-0.5	elliptic to circular	$s_0 = 0.4013$ $\dot{s}_0 = -0.1$ $\theta_0 = 0$ $L_{z0} = 0.8$	1	48.8

Table III. Examples of transfers with constant effective energy. All the quantities are dimensionless, except the θ_0 which is measured in radians.

a sequence of three transfers: 1) with increasing energy and constant angular momentum, 2) with constant energy and decreasing angular momentum and 3) with decreasing energy and constant angular momentum. Under these conditions, all the transfers have stable bounded orbits.

So, the control conditions to transfers with $L_{z0} < L_{zf}$ are

$$H > 0, L_{z0} < L_{zf}: \begin{cases} \text{if } \dot{s} > 0 \wedge L_{z0} < L_{zf} \Rightarrow \sigma = 1 \\ \text{otherwise } \Rightarrow \sigma = 0 \end{cases}$$
$$H < 0, L_{z0} < L_{zf}: \begin{cases} \text{if } \dot{s} > 0 \wedge L_{z0} < L_{zf} \Rightarrow \sigma = 1 \\ \text{if } \dot{s} = 0 \wedge s \in [s_1^*, s_0^*] \wedge L_{z0} < L_{zf} \Rightarrow \sigma_c = 0 \\ \text{otherwise } \Rightarrow \sigma = 0 \end{cases} \quad (20)$$

Some examples of these transfers are indicated in Table III. However, since the effective energy remains constant during all the transfer, the satellite can only be transferred between closed ($H < 0$) or open ($H > 0$) orbits.

In Figure 2, we simulate the transfer of a satellite starting in an initial elliptic orbit with angular momentum $L_{z0} = 0.8$ to the circular orbit with radius $s = 1$ and effective energy $H = -0.5$ (angular momentum $L_{zf} = 1$). The main characteristics of this transfer are summarized in the last example of Table III. In this figure are presented trajectories of phase and configuration spaces as well as the control parameter, angular momentum, and effective energy variations. This example is more complex than the others presented because the circular orbit is not directly reachable and we had to implement the

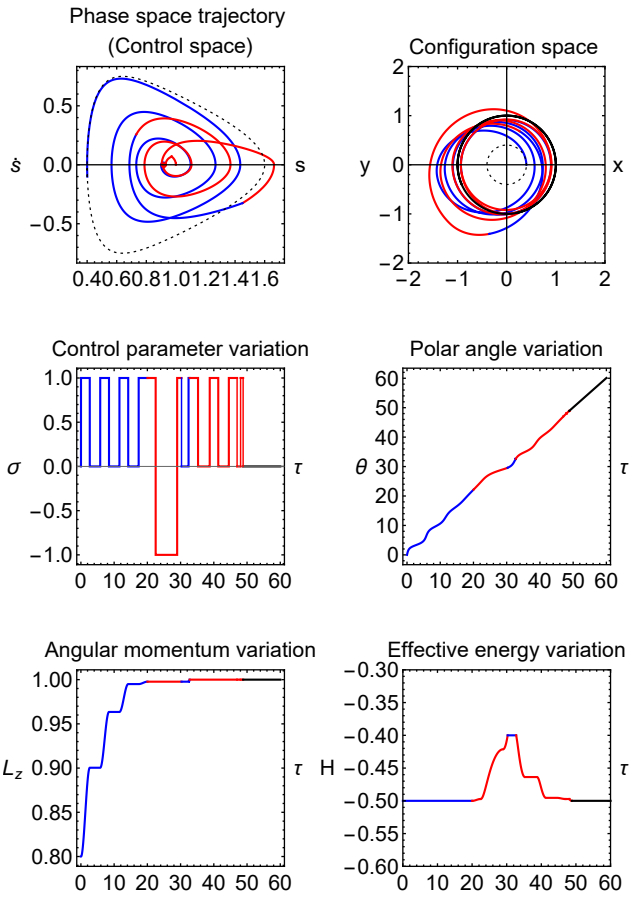

Figure 2. Simulation of a transfer with constant effective energy between elliptic and circular Keplerian orbits with $H_0 = -0.5$. The initial and final angular momenta are $L_{z0} = 0.8$ and $L_{zf} = 1$, respectively. The transfer starts at the point $(s_0, \dot{s}_0) = (0.4013, -0.1)$ and $\theta_0 = 0$. The initial orbit is represented by the dashed line, constant effective energy transfers by blue lines, constant angular momentum transfers by red lines and the final orbit by the black line. The normalized transfer time is $\Delta\tau = 48.8$.

strategy previously defined. First of all, we transfer the satellite to an almost circular orbit with constant effective energy, and when $s_1^* < s < s_0^*$ and $\dot{s} = 0$ are reached, we start a transfer with increasing effective energy and constant angular momentum (similar to those studied in the previous chapter) until a value relatively close to H is reached, which in this case was $H = -0.4$. When this happens, a transfer with constant effective energy and decreasing angular momentum is started and it ends when L_{zf} is reached. After this, the satellite is transferred with decreasing effective energy and constant angular momentum until the circular orbit by the method described in the last section III. The normalized total time of this transfer is $\Delta\tau = 48.8$.

V. Transfers with both variable angular momentum and effective energy

Now we consider transfers with both variable angular momentum and effective energy. We want to make a transfer between an orbit with L_{z0} and H_0 and another with L_{zf} and

H_f. Thus, we can have four cases: i) $H_0 < H_f$ and $L_0 < L_f$, ii) $H_0 > H_f$ and $L_0 < L_f$, iii) $H_0 < H_f$ and $L_0 > L_f$ and iv) $H_0 > H_f$ and $L_0 > L_f$.

There are two different ways to obtain these transfers. The first consists of grouping transfers with constant effective energy with transfers with constant angular momentum exactly as described in the previous sections; the second is obtained through conservation laws.

For the first case, we combine transfers with constant angular momentum and transfers with constant effective energy. Therefore, for each one of the four cases mentioned above, we can have two ways of making this:

a) making a transfer with constant L_z followed by a transfer with constant H;

b) making a transfer with constant H followed by a transfer with constant L_z.

Using the control conditions mentioned in sections III and IV, we obtained some simulation transfers between circular, elliptical, and hyperbolic orbits to each one of the four possible cases - i) to iv) - and with the two possible transfer combinations - a) and b). These results are summarized in Table IV.

Note cases i) and iv), where both angular momentum and effective energy increase or decrease, and when the transfer involves a circular orbit, there only is a way to implement the transfer. When $H_0 < H_f$ and $L_{z0} < L_{zf}$, case i), we were unable to transfer the satellite to a circular orbit by first implementing a transfer to constant effective energy followed by another with constant angular momentum because in the first the minimum energy value (circular orbit) is exceeded. The problem in case iv) is similar to this. When $H_0 > H_f$ and $L_{z0} > L_{zf}$, if the satellite is in a circular orbit and we want to transfer it to any other orbit, it will only be possible if we first implement a transfer with constant H followed by another with constant L_z. Otherwise, the minimum energy value will be exceeded and this is not physically possible. This will be discussed in detail in section VI.

In the examples presented, the final orbit orientation is once again different from the initial orbit. The technique described in section VII to rotate the final orbit can also be used in this case.

Figure 3 shows an example of a transfer simulation with both increasing effective energy and angular momentum: a transfer between elliptical and hyperbolic orbits. The initial and final conditions are referenced in the first example in Table IV. First, we apply for a constant effective energy transfer and then another with constant angular momentum. However, on the plot of the effective energy variation in the same figure, we observe two transfers with constant angular momentum (red lines) and another two with constant effective energy (blue lines). This is due to the fact that the satellite enters the problematic region studied in section IV. To solve this, we implement the strategy described in that section to the circular orbits (which includes three more types of transfers) but we stop it when the desired angular momentum value L_{zf} is reached. Only after that the transfer with constant L_z begins

case	initial conditions	final conditions	$\Delta\tau$
i)	$s_0 = 1.1857$ $\dot{s}_0 = -0.25$ $\theta_0 = 0$ $H_0 = -0.3$ $L_{z0} = 1.2$	$H_f = 0.1$ $L_{zf} = 1.5$	$\Delta\tau_a = 8.9$ $\Delta\tau_b = 24.7$
i)	$s_0 = 0.8$ $\dot{s}_0 = -0.5$ $\theta_0 = 0$ $H_0 = -0.3438$ $L_{z0} = 1$	$H_f = -0.3$ $L_{zf} = 1.2909$	$\Delta\tau_a = 52.5$ b) inaccessible
ii)	$s_0 = 0.1878$ $\dot{s}_0 = -0.2$ $\theta_0 = \pi$ $H_0 = 0.2$ $L_{z0} = 0.6231$	$H_f = -0.5$ $L_{zf} = 1$	$\Delta\tau_a = 76.7$ $\Delta\tau_b = 61.1$
iii)	$s_0 = 2.25$ $\dot{s}_0 = 0$ $\theta_0 = 0$ $H_0 = -0.2222$ $L_{z0} = 1.5$	$H_f = -0.1$ $L_{zf} = 0.9$	$\Delta\tau_a = 7.1$ $\Delta\tau_b = 8.95$
iv)	$s_0 = 0.4148$ $\dot{s}_0 = -0.1$ $\theta_0 = 0$ $H_0 = 0.5$ $L_{z0} = 1$	$H_f = 0.2$ $L_{zf} = 0.8$	$\Delta\tau_a = 3.2$ $\Delta\tau_b = 4.4$
iv)	$s_0 = 1$ $\dot{s}_0 = 0$ $\theta_0 = 0$ $H_0 = -0.5$ $L_{z0} = 1$	$H_f = -0.7$ $L_{zf} = 0.8$	a) inaccessible $\Delta\tau_b = 8.5$

Table IV. Examples of transfers with both varying angular momentum and effective energy.

and takes $\Delta\tau = 38.5$ (normalized time). In fact, in this particular case, the first transfer takes a normalized time $\Delta\tau = 17.1$ and includes an initial transfer with constant H until $\dot{s} = 0$ and $s_1^* < s < s_0^*$, another with constant L_z up to a chosen value close to H_0 (in this case $H = -0.2$) followed by another with constant H until the final value L_{zf}. Therefore, the total normalized transfer time is $\Delta\tau = 55.6$.

The second hypothesis to compute transfers with both variable angular momentum and effective energy uses control conditions given by the conservation laws. If we plot the ef-

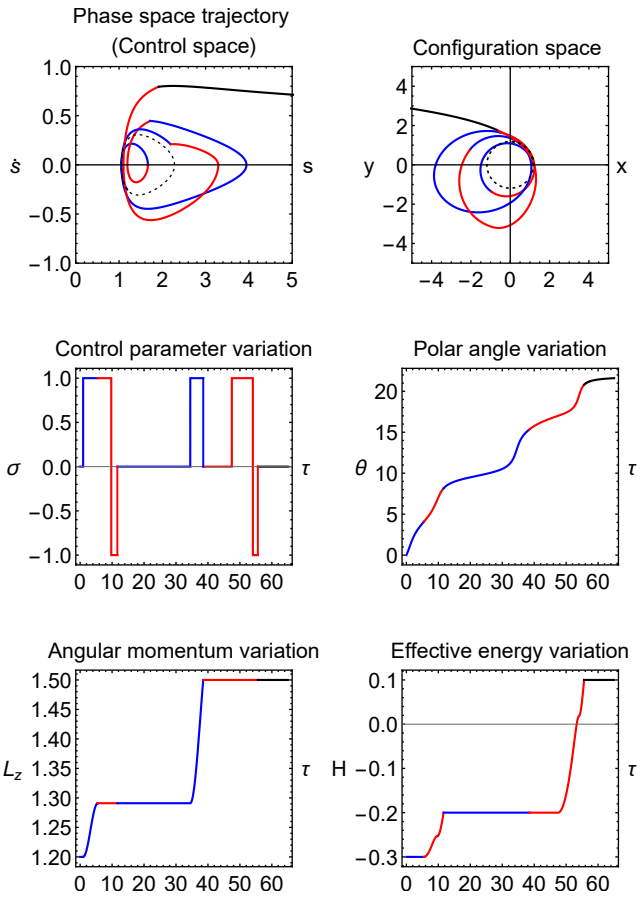

Figure 3. Simulation of a transfer with both varying angular momentum and effective energy between elliptical and hyperbolic orbits: the initial one with $L_{z0} = 1.2$ and $H_0 = -0.3$ and the final with $L_{zf} = 1.5$ and $H_f = 0.1$. The initial orbit is represented by the dashed line, the first transfer (with constant H) by the blue line, the second transfer (with constant L_z) by the red line and the final orbit by the black one. The transfer starts at the point $(s_0, \dot{s}_0, \theta_0) = (1.1857, -0.25, 0)$. The normalized transfer time is $\Delta\tau = 55.6$.

fective energy as a function of the angular momentum of any of the transfers studied so far, we see this is a straight segment with a slope k. So, we can write

$$\frac{dH}{dL_z} = \frac{H_f - H_0}{L_{zf} - L_{z0}} = k, \tag{21}$$

where k is a constant that can be positive or negative according to the case we are analyzing. $k > 0$ if L_z and H increase or decrease; $k < 0$ if one increases and the other decreases. Therefore, this new equation is the other condition that will help us to implement these transfers.

We know that the equations that describe these transfers are given by (6) and (8):

$$\begin{cases} \ddot{s} = \frac{L_z^2}{s^3} - \frac{1}{s^2} + \varepsilon\sigma\cos(\theta - \phi) \\ \dot{L}_z = -\varepsilon\sigma s\sin(\theta - \phi) \\ \dot{H} = \varepsilon\sigma\left[\dot{s}\cos(\theta - \phi) - s\dot{\theta}\sin(\theta - \phi)\right], \end{cases} \tag{22}$$

If we replace the last two equations of (22) in (21), we obtain $\tan(\theta - \phi) = \dot{s}/(s\dot{\theta} - ks)$, and if we still replace these equations in (22) we have the final equations to use in transfer simulations:

$$\begin{cases} \ddot{s} = \frac{L_z^2}{s^3} - \frac{1}{s^2} + \varepsilon\sigma\frac{s\dot{\theta} - ks}{\left[\dot{s}^2 + (s\dot{\theta} - ks)^2\right]^{\frac{1}{2}}} \\ \dot{L}_z = -\varepsilon\sigma s\frac{\dot{s}}{\left[\dot{s}^2 + (s\dot{\theta} - ks)^2\right]^{\frac{1}{2}}} \\ \dot{H} = -\varepsilon\sigma s\frac{\dot{s}k}{\left[\dot{s}^2 + (s\dot{\theta} - ks)^2\right]^{\frac{1}{2}}} = k\dot{L}_z \\ \dot{\theta} = \frac{L_z}{s^2} \end{cases} \tag{23}$$

Note that these transfers have both effective energy and angular momentum variable and for each one of the four possible cases it is still necessary to impose other conditions: i) when $s\dot{s} > 0$ implies $\sigma = 1$ and $s\dot{s} < 0$, $\sigma = -1$, and ii) when $s\dot{s} > 0$ implies $\sigma = -1$ and $s\dot{s} < 0$, $\sigma = 1$.

We present an example of this type of transfers for the case ii) - Figure 4. However, we have not yet been able to obtain transfer simulations for any values of H and L_z because there are still problematic regions (close to the fixed points). This may imply a different choice of control parameters, but we leave our suggestion for possible future work on this subject. Besides, we also call for the study of these transfers when one of the quantities (H or L_z) increases, and the other decreases. This type of transfers may be important since they are more efficient than those studied at the beginning of this section.

VI. Transfers between two circular orbits

In Figure 5 are represented schematically all types of transfers carried out until now:

1. transfer with constant angular momentum (Section III);
2. transfer with constant effective energy (Section IV);
3. transfer with both variable angular momentum and effective energy (Section V);

and also the method of transfers between two circular orbits that we are studying in this section, depicted by the orange line.

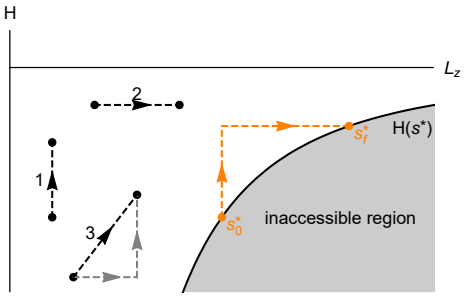

Figure 5. Effective energy diagram as a function of the angular momentum of the various transfers simulated in this project.

Still in Figure 5 is represented by the solid black line all the possible circular orbits, which coincides with the fixed point $(s, \dot{s}) = (s_0^*, 0)$ and the angular momentum and effective energy expressions are $L_z(s_0^*, 0) = \sqrt{s_0^*}$ and $H(s_0^*) = -1/(2s_0^*)$, respectively. Since the black line corresponds to circular orbits and since they have the possible minimum energy, the

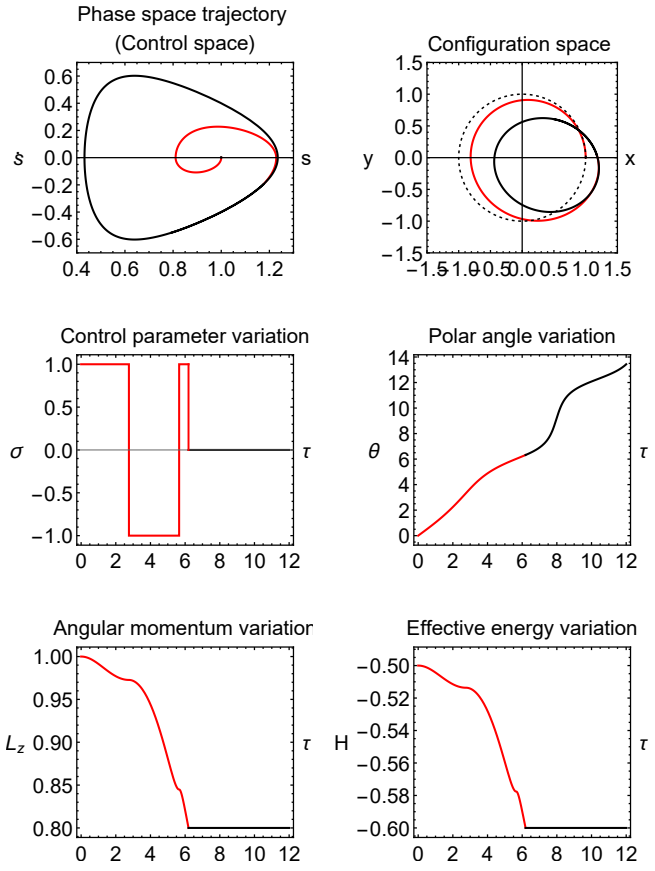

Figure 4. Simulation of a transfer with angular momentum and effective energy both variable between a circular and an elliptical orbits: the initial with $L_{z0} = 1$ and $H_0 = -0.5$ and the final with $L_{zf} = 0.8$ and $H_f = -0.6$. The initial orbit is represented by the dashed line, the first transfer (with both variable H and L_z) by the blue line, the second transfer (with constant H) by the red line and the final orbit by the black one. The transfer starts at the point $(s_0, \dot{s}_0, \theta_0) = (1,0,0)$ and its normalized time is $\Delta\tau = 6.2$.

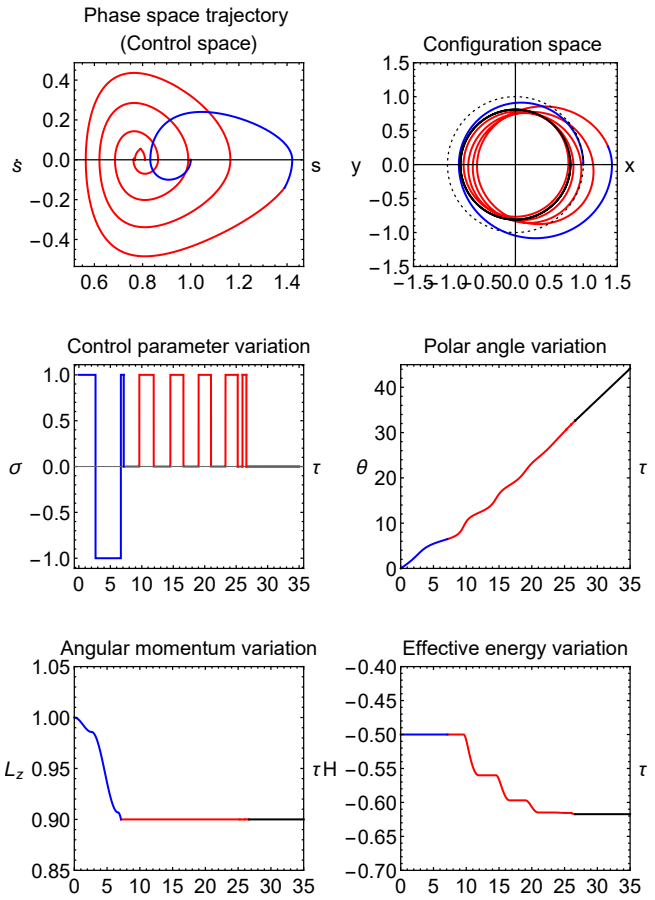

Figure 6. Simulation of a transfer with both variable angular momentum and effective energy between two circular orbits $s_0 > s_f$: the initial with $L_{z0} = 1$ and $H_0 = -0.5$ and the final with $L_{zf} = 0.9$ and $H_f = -0.6173$. The initial orbit is represented by the dashed line, the first transfer (with constant H) by the blue line, the second (with constant L_z) by the red line and the final orbit by the black one. The transfer starts at the point $(s_0, \dot{s}_0) = (1,0)$ with $\theta_0 = 0$. The transfer time is $\Delta\tau = 26.6$ (dimensionless).

gray region is not accessible and it is impossible to simulate transfers there. This way, it is now possible to understand why for transfers with constant effective energy it is necessary that $H \geq -1/(2L_{z0}^2)$ if $L_{z0} > L_{zf}$ and $H \geq -1/(2L_{zf}^2)$ if $L_{zf} > L_{z0}$.

From here, we conclude that, to obtain transfers between two circular orbits, both effective energy and angular momentum must increase/decrease simultaneously as the radius of the final orbit increases/decreases relative to the initial one.

Considering the two orange points represented in the figure as the initial and final points of a transfer between two circular orbits, it is obvious that the most effective way to obtain the endpoint would be to follow the trajectory of the continuous black line that joins the two points. However, this is not possible with using the numerical method of integration Runge-Kutta 4^{th} order because it does not allow us to obtain such an exact result.

Through the scheme represented in Figure 5, we conclude that the order of transfers to be implemented is:

i) a constant effective energy transfer followed by a constant angular momentum transfer if $s_0 > s_f$;

ii) a constant angular momentum transfer followed by a constant effective energy transfer if $s_f > s_0$.

Note that in the latter case, when we apply for transfers with constant effective energy, we implement the strategy described in section IV and, therefore, it is not just a transfer to constant H but three different transfers interchanged between transfers with constant H and transfers with constant L_z.

In Figure 6 we present an example of a transfer simulation between two circular orbits through the implementation of method i) where $s_0 > s_f$. The initial orbit is characterized by $L_{z0} = 1$ and $H_0 = -0.5$ and the final one by $L_{zf} = 0.9$ and $H_f = -0.6173$. The transfer starts at the point $(s_0, \dot{s}_0 = 1,0)$ with $\theta_0 = 0$ and it takes 26.6 (dimensionless) to be completed. The control parameter variation σ has a different definition depending on the type of transfer, following the control choices of section III during the constant angular momentum transfer (red line) and of section IV during the constant effective energy transfer (blue line).

VII. Final orbit rotation through the Laplace-Runge-Lenz vector

As described by the examples given in the previous chapters, after a transfer, the final orbit rotates relative to the initial one. This is true both for transfers with constant angular momentum as well as for transfers with constant effective energy.

Since it is a constant of motion of the Kepler problem, the LRL vector is invariant for any point in a certain orbit and is calculated using equation (10). In this way, we can calculate the LRL vectors for the initial and final orbits and the scalar product of these two vectors allows us to discover the angle of rotation $\Delta\alpha$ between the orbits:

$$\Delta\alpha = \arccos\left[\frac{A_{x0}A_{xf} + A_{y0}A_{yf}}{\left(A_{x0}^2 + A_{y0}^2\right)^{\frac{1}{2}}\left(A_{xf}^2 + A_{yf}^2\right)^{\frac{1}{2}}}\right], \qquad (24)$$

where A_{x0} and A_{y0} are the components of the LRL vector relative to the initial orbit, and A_{xf} and A_{yf} are also the components of the LRL vector but relative to the final orbit.

Since we want the final orbit to have the same orientation as the initial one, we have to rotate the final orbit by an angle $-\Delta\alpha$. Depending on the case we are considering, we use transfers with constant angular momentum or transfer with constant effective energy and we turn the control on with $\sigma = 1$ at a point $(s_r, \dot{s}_r)$ of the final orbit and turn it off when $(s_r, -\dot{s}_r)$ is reached. The phase space is invariant under rotations but we reach a Keplerian orbit defined by the same angular momentum and energy as the initial one with a different orientation, which means that the orbit precesses in configuration space but rarely at the desired angle $-\Delta\alpha$. Then, so that the orbits have the same orientation, it is necessary to find the initial angle θ_r that satisfies these conditions. This method can be applied for the rotation of elliptical and hyperbolic Keplerian orbits.

To better understand the orbits trajectory in the phase and configurations spaces, we have to consider two cases: i) $\dot{s}_r > 0$ and ii) $\dot{s}_r < 0$. In Figure 7 are presented these two cases. On the top, after a transfer with constant angular momentum, we turn on the control $\sigma = 1$ when $\dot{s}_r > 0$ and $\theta_r = 3.4629$ and we rotate the final orbit (black). The rotated orbit is represented in orange. In the plots below, we have a similar situation but we started to rotate the orbit after a transfer with constant effective energy. The control is turned on when $\dot{s}_r < 0$ and with $\theta_r = 3.9021$. However, comparing the LRL vectors (black and orange) we concluded that, in both cases, the rotated orbit didn't rotate enough to align the vectors. Thus, we see a precession in the configuration space, which means that we can change its orientation continuously, depending on the chosen θ_r angle.

Manipulating the initial polar angle we find the θ_r that leads to a rotation of the final orbit with the desired angle $-\Delta\alpha$. Thus, to the examples we are considering, these values are $\theta_r = 2.8575$ and $\theta_r = 3.8265$. Thus, the process is complete and we obtain a transfer with constant angular momentum and with constant effective energy, where the initial and final orbits have the same orientation, using the constants of motion of the Kepler problem. This is depicted in Figure 8.

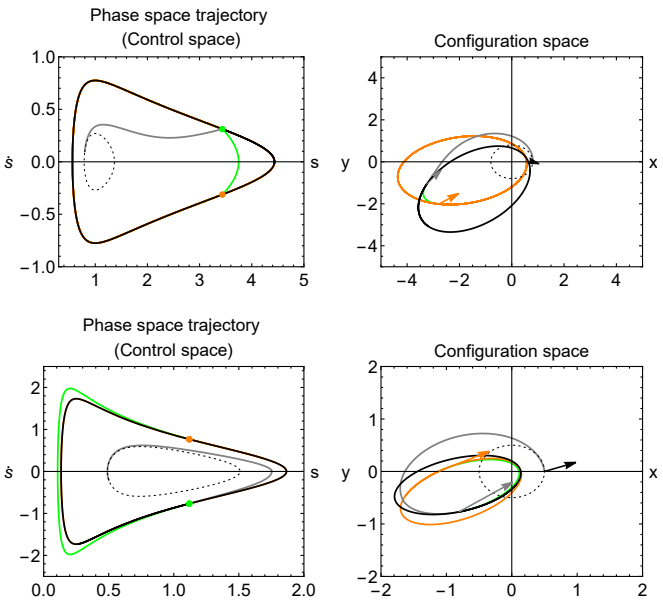

Figure 7. Simulation of the implemented method to rotate an orbit. On the top, the control is turned on the control with $\sigma = 1$ at the point $(s_r, \dot{s}_r) = (3.4375, 0.3118)$ with $\theta = 3.4629$ and is turned off when the point $(s, \dot{s}) = (s_r, -\dot{s}_r)$ is reached. The angular momentum remains constant and are $L_z = 1$. On the bottom, the control is turned on the control at the point $(s_r, \dot{s}_r) = (1.1194, -0.7663)$ with $\theta_r = 3.9021$ and is turned off when the point $(s, \dot{s}) = (s_r, -\dot{s}_r)$ is reached. The effective energy remains constant ($H = -0.5$). The green lines correspond to the orbit trajectory change while control parameter is on and the oranges to the rotate final orbits. On the left plots, the black and orange orbits coincide.

Note that, with this method, it is not possible to measure the time it takes to obtain an orbit with the desired orientation. We are only able to discover one condition (in this case the initial polar angle) for this to happen. We can only know, for any θ_r, how long it takes from the moment we start to rotate the orbit until it has the desired orientation. This value is constant and independent of the θ_r value. In these cases, it corresponds to 4.0 to the first one and to 1.7 to the second.

VIII. Conclusions

The main goal of this project was to develop a control strategy to be applied in satellites' low-thrust transfers between two-dimensional Keplerian orbits through conservation laws. We started by presenting the mathematical formalism of the two-dimensional Kepler problem with varying mass, where the reference frame (centered at the primary body) is inertial in the limit $m/M \to 0$. Assuming that the thrusters exhaust gases intensity are constant, we obtained the equations of motion for this problem, which has three constants of motion: the angular momentum vector, the effective energy, and the Laplace-Runge-Lenz vector. However, during transfers, they are no longer constants. This means that, the satellite is initially in an initial orbit with a certain angular momentum, effective energy, and LRL vector. When the control is turned on, one or two of these constants (depending on the type of

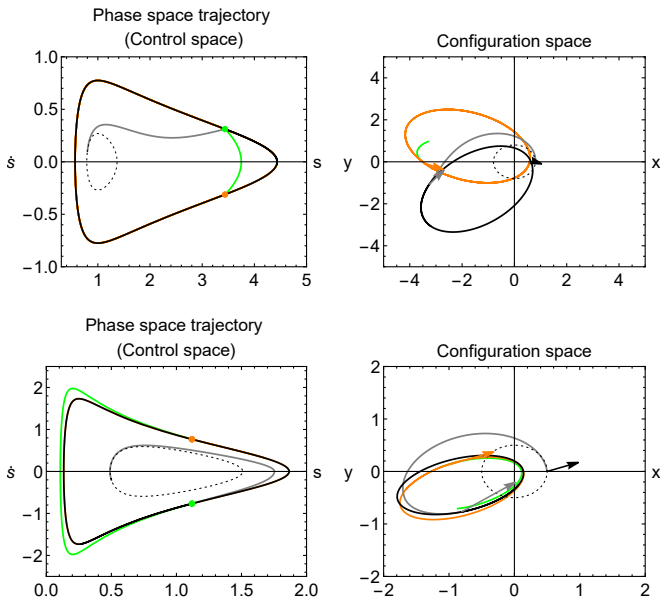

Figure 8. On the top, rotation of an orbit resulting from a transfer with constant angular momentum ($L_z = 0.8$). The rotation is also done with constant angular momentum. The initial conditions are $(s_r, \dot{s}_r, \theta_r) = (3.4375, 0.3118, 2.8575)$ and it takes 4.0 to reach the point $(s_r, -\dot{s}_r)$. On the bottom, rotation of an orbit resulting from a transfer with constant effective energy ($H = -0.5$). The rotation is also done with constant effective energy. The initial conditions are $(s_r, \dot{s}_r, \theta_r) = (1.1194, -0.7663, 3.8265)$ and it takes 1.7 to reach the point $(s_r, -\dot{s}_r)$. The initial and final orbits are represented by the dashed and black lines, respectively, and the rotated orbit by the orange line. In green (left plot), the phase space is shown when the control is on, and it is confirmed that when it is turned off, we remain in the same orbit but with a different orientation (right plot).

transfer we are considering) are no longer constant and the satellite moves to another orbit. When the desired value is reached, the control turns off and we have the three constants of motion again but now with different values according to the final orbit.

Transfers can be between circular, elliptical, or hyperbolic orbits. Besides, they can start at any point in the orbit. We simulated transfers with constant angular momentum, with constant effective energy, and with both these quantities both variable. The latter results from the combination of the first two transfers and also from a more efficient method using only conservation laws. However, this method is not yet totally completed because some problems related to the regions near the fixed points were not being solved. We encourage anyone who wants to study this topic to explore this method as it is more efficient than the first one since both angular momentum and effective energy vary simultaneously. We also simulated a particular type of transfers: between two circular orbits. For each transfer, we used different control choices depending on its phase space. We used a *bang-bang* control, where the parameter control, σ, could only be ± 1 or 0, in which the latter corresponds to the control being turned off.

In both types of transfers with constant angular momentum and with constant effective energy, due to the orbital phase spaces, it was not possible to reach directly the circular orbit. To solve this, we had to implement new strategies described in the final of sections III and IV.

After transfers with constant angular momentum or with constant effective energy, the LRL vector was used to rotate the final orbit until it was oriented exactly like the initial one.

For future work, in addition to the suggestions mentioned above, we propose two more topics: the simulation of a real transfer, using known thrust parameters as well as the implementation of a similar strategy to three-dimensional transfers.

[1] D. F. Lawden, *Advances in Space Science - Interplanetary Rocket Trajectories*. Academic Press, 1959. vol. 1.

[2] H. Munick, R. McGill, and G. E. Taylor, "Analytic Solutions to Several Optimum Orbit Transfer Problems," *Journal of the Astronautical Sciences*, vol. 7, no. 4, pp. 73–77, 1960.

[3] T. N. Edelbaum, "Propulsion Requirements for Controllable Satellites," *ARS Journal*, vol. 32, no. 8, p. 1079–1089, 1961.

[4] J. Gergaud and T. Haberkorn, "Homotopy Method for Minimum Consumption Orbit Tranfer Problem," *ESAIM: Control, Optimisation and Calculus of Variations*, vol. 12, p. 294–310, February 2005.

[5] S. Lee, P. von Allmen, W. Fink, A. E. Petropoulos, and R. J. Terrile, "Design and Optimization of Low-Thrust Orbit Transfers," *IEEE Aerospace Conference*, 2005.

[6] A. L. Herman and D. B. Spencer, "Optimal, Low-Thrust Earth-Orbit Transfers Using Higher-Order Collocation Methods," *Journal of Guidance, Control, and Dynamics*, vol. 25, no. 1, January–February 2002.

[7] W. Hohmann, *The Attainability of Heavenly Bodies*. National Aeronautics and Space Administration (NASA), 1960 (technical translation).

[8] W. D. Dickerson and D. B. Smith, "Trajectory Optimization for Solar-Electric Powered Vehicles," *AIAA Paper 67-583*, August 1967.

[9] R. Dudney, "Rescue in Space," *Air Force Magazine*, p. 38–41, January 2012.

[10] R. Killinger, R. Kukies, M. Surauer, A. Tomasetto, and L. van Holtz, "ARTEMIS Orbit Raising Inflight Experience with Ion Propulsion," *Acta Astronautica*, vol. 53, no. 4, p. 607–621, 2003.

[11] S. Zhao and J. Zhang, "Minimum-Fuel Station-Change for Geostationary Satellites Using Low-Thrust Considering Perturbations," *Acta Astronautica*, p. 296–307, October–November 2016.

[12] M. da Silva Fernandes, "Orbit Transfers Between Keplerian Orbits," Master's thesis, Instituto Superior Técnico, October 2017.

[13] R. Dilão, M. Fernandes, and M. Sá, "Low-Thrust Orbit Transfers Between Two-Body Keplerian Orbits," *Preprint*, December 2020.

[14] H. Goldstein, C. Poole, and J. Safko, *Classical Mechanics*. Addison Wesley, 2002 (3rd edition).

[15] R. Dilão, *Uma Introdução Informal à Teoria dos Sistemas Dinâmicos e do Caos*. 2016.